The Effect of Fat Pad Modification during Ablation of Atrial Fibrillation: Late Gadolinium Enhancement MRI Analysis

KOJI HIGUCHI, M.D., MEHMET AKKAYA, M.D., MATTHIAS KOOPMANN, M.D., JOSHUA J.E. BLAUER, B.Sc., NATHAN S. BURGON, B.Sc., KAVITHA DAMAL, Ph.D., RAVI RANJAN, M.D., Ph.D., EUGENE KHOLMOVSKI, Ph.D., ROB S. MACLEOD, Ph.D., and NASSIR F. MARROUCHE, M.D.

From the Comprehensive Arrhythmia and Research Management (CARMA) Center, University of Utah School of Medicine, Salt Lake City, Utah

Background: *Magnetic resonance imaging (MRI) can visualize locations of both the ablation scar on the left atrium (LA) after atrial fibrillation (AF) ablation and epicardial fat pads (FPs) containing ganglionated plexi (GP).*

Methods: *We investigated 60 patients who underwent pulmonary vein antrum (PVA) isolation along with LA posterior wall and septal debulking for AF. FPs around the LA surface in well-known GP areas (which were considered as the substitution of GP areas around the LA) were segmented from the dark-blood MRI. Then the FP and the ablation scar image visualized by late gadolinium enhancement (LGE)-MRI on the LA were merged together. Overlapping areas of FP and the ablation scar image were considered as the ablated FP areas containing GP. Patients underwent 24-hour Holter monitoring after ablation for the analysis of heart rate variability.*

Results: *Ablated FP area was significantly wider in patients without AF recurrence than those in patients with recurrence (5.6 ± 3.1 cm^2 vs 4.2 ± 2.7 cm^2, $P = 0.03$). The mean values of both percentage of differences greater than 50 ms in the RR intervals (pRR > 50) and standard deviation of RR intervals over the entire analyzed period (SDNN), which were obtained from 24-hour Holter monitoring 1-day post-AF ablation, were significantly lower in patients without recurrence than those in patients with recurrence ($5.8 \pm 6.0\%$ vs $14.0 \pm 10.1\%$; $P = 0.0005$, 78.7 ± 32.4 ms vs 109.2 ± 43.5 ms; $P = 0.005$). There was a significant negative correlation between SDNN and the percentage of ablated FP area ($Y = -1.3168X + 118.96$, $R^2 = 0.1576$, $P = 0.003$).*

Conclusion: *Extensively ablating LA covering GP areas along with PVA isolation enhanced the denervation of autonomic nerve system and seemed to improve procedural outcome in patients with AF. (PACE 2013; 00:1–10)*

ganglionated plexi, fat pad, atrial fibrillation, catheter ablation, LGE-MRI

Introduction

The primary procedure of catheter ablation for atrial fibrillation (AF) is electrical isolation of pulmonary veins (PVs).[1,2] Many groups have demonstrated that late gadolinium enhancement magnetic resonance imaging (LGE-MRI) can visualize the extent of scar after radiofrequency (RF) ablation on the left atrial (LA) wall[3–6] using slow washout kinetics of the gadolinium-based contrast agents in the regions of non-viable or scarred myocardium.[7,8] Experimental and clinical data suggest that the autonomic nervous system (ANS), including ganglionated plexi (GP), may play a critical role in AF.[9–12] Several studies indicated that ablating GP along with PV isolation may significantly decrease AF recurrences postablation.[13–15] These GP areas reside within epicardial fat pads (FPs) near PV-LA junctions and around Marshall Vein; thus, lesions after PV antrum (PVA) isolation automatically include these GP areas. Therefore, the autonomic denervation after PVA isolation enhances the long-term benefit of PVA isolation.[16]

On the basis of the importance of ablating GP areas during AF ablation, we sought to evaluate the impact of ablating FP areas containing GP on the result of AF ablation using postablation MRI.

Methods

Study Population

Between May 2009 and January 2011, 159 patients underwent AF ablation at the University of Utah. These patients were retrospectively examined. We selected the population of this study according to the following criteria: patients who underwent (1) an excellent quality LGE-MRI (for the assessment of lesion created by ablation) 3-month post-AF ablation, (2) a dark-blood MRI without fat suppression (for the assessment of FP areas containing GP around the LA) 3-month post-AF ablation, (3) a 24-hour Holter monitoring 1-day postablation (to evaluate the heart rate variability postablation). We found 60 consecutive patients (35 men, 65 ± 13 years old) who met these criteria in these 159 patients and they were included in this study.

Ablation Procedure

The PVA isolation procedure with LA posterior wall and septal wall debulking has been described.[4,17,18] The LA was accessed through two transseptal punctures under intracardiac echo catheter guidance (Acunav, Siemens Medical Solutions USA, Inc., Mountain View, CA, USA). A 10-pole circular mapping catheter (Lasso, Biosense Webster, Diamond Bar, CA, USA) and a 3.5-mm irrigated-tip ablation catheter (Thermocool, Biosense Webster) were advanced into the LA. Lesions were created using RF energy of 50 W with tip temperature of $50°C$ for no longer than 5 seconds with the guidance of 3D electroanatomical mapping with CARTO (Biosense Webster).

Electrical isolations of all PVs were achieved first, in which ablation lesions were placed in a circular fashion along the PVA until PV electrograms were eliminated. The bidirectional block was also confirmed by pacing in each PV to ensure the complete electrical isolation of each PV.

Afterwards intracardiac potentials in the PVA region, on the LA posterior wall, and on the LA septum wall were mapped during sinus rhythm. If fractionations were seen distinct from far-field atrial potentials recorded on Lasso electrogram placed on these areas, they were targeted for ablation as a substrate of AF. The endpoint of RF delivery was abolition of local electrograms recorded on the Lasso catheter.

MRI Image Acquisition

LGE-MRI studies were performed on a 1.5 Tesla Avanto scanner (Siemens Healthcare, Erlangen, Germany) to assess the postablation scarring on the LA wall.[3,4] The scan was acquired about 15 minutes following contrast agent injection (0.1 mmol/kg, Multihance [Bracco Diagnostic Inc., Princeton, NJ, USA]) using a 3D inversion recovery, respiration navigated, electrocardiogram (ECG)-gated, gradient echo pulse sequence. Acquisition parameters were: free-breathing using navigator gating, a transverse-imaging volume with field of view $= 360 \times 360 \times 110$ mm, imaging matrix $= 288 \times 288 \times 44$, voxel size $= 1.25 \times 1.25 \times 2.5$ mm (reconstructed to $0.625 \times 0.625 \times 1.25$ mm), repetition time/echo time $= 5.4/2.3$ ms, flip angle $= 20°$, inversion time $= 270–310$ ms. ECG gating was used to acquire a small subset of phase-encoding views during the diastolic phase of the LA cardiac cycle. The time interval between the R-peak of the ECG and the start of data acquisition was defined using the cine images of the LA. Dark-blood images were acquired prior to the contrast agent injection during the same MRI session. These images were acquired using 2D double-inversion-prepared, respiration-navigated, ECG-gated, turbo spin echo pulse sequence with the following parameters: contiguous transverse imaging slices, field of view $= 360 \times 360$ mm, slice thickness of 4 mm, imaging matrix $= 288 \times 288$, pixel size $= 1.25 \times 1.25$ mm (interpolated to 0.625×0.625 mm), repetition time $=$ one heartbeat, echo time $= 61$ ms, echo-train length $= 22$.

LA Wall Segmentation and Assessment of Postablation Scarring

LA wall was manually segmented from the LGE-MRI images using the Corview image processing software (MARREK Inc., Salt Lake City, UT, USA). Images of postablation scarring were acquired from LA wall enhancement using a threshold-based lesion detection algorithm as described previously.[3] We used an unsupervised statistical clustering algorithm on normalized pixel intensities to define the distribution of image enhancement due to scar and to separate enhancement from normal tissue.

Definition of GP Areas

We used FP areas containing GP for the surrogate of GP areas. Therefore, we defined GP areas surrounding LA carefully by reference to previous studies.

There are five GP areas around LA: superior left GP (SLGP) area, inferior left GP (ILGP) area, anterior right GP (ARGP) area, inferior right GP (IRGP) area, and Marshall GP (MGP) area.[11,13–15,19–22] Detailed anatomic locations of GP were based on previous reports from the autonomic innervation of human heart[19,20,22–24] and experiences of other investigators who identified GP by means of high-frequency stimulation (HFS).[11,14,25] We followed these anatomic instructions and defined certain GP areas as shown in
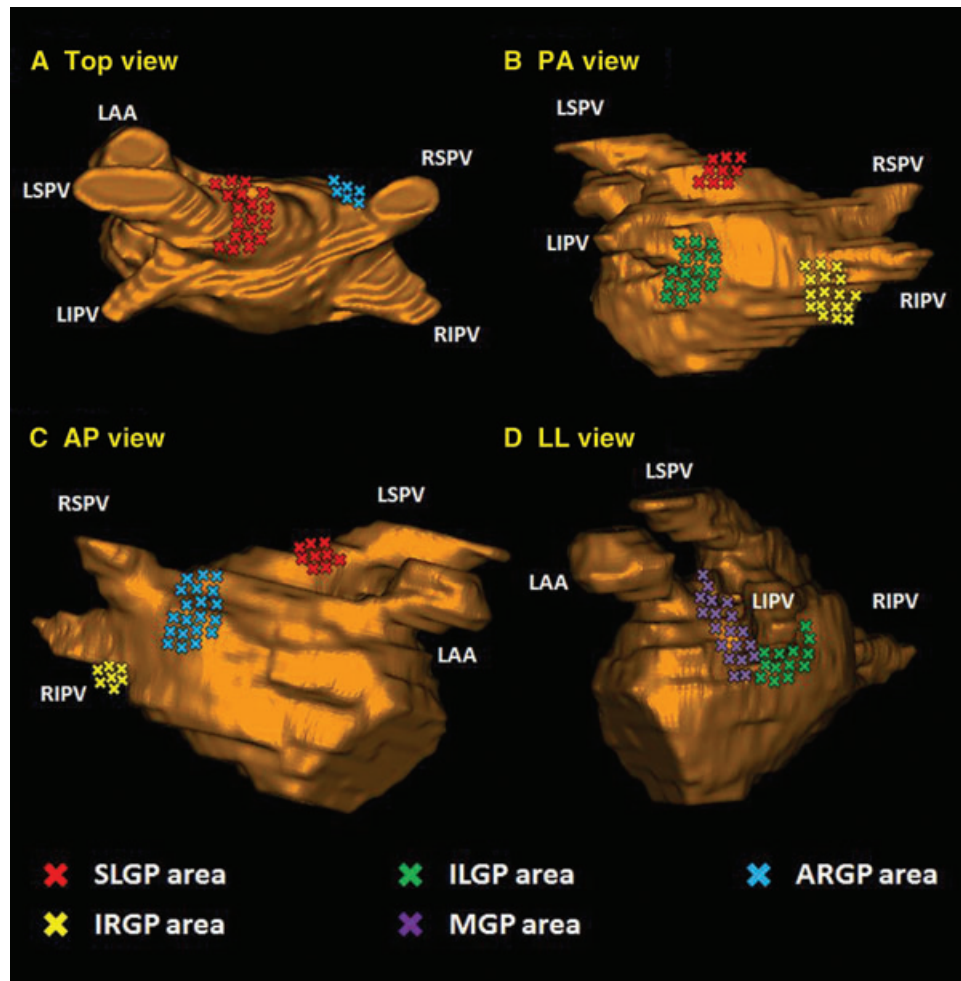
Figure 1. *This figure shows the schematic image of the location of each GP area displayed on the LA image. Red, green, blue, yellow, and purple cross-mark correspond with SLGP, ILGP, ARGP, IRGP, and MGP areas, respectively. AP = anterior posterior; ARGP = anterior right GP; GP = ganglionated plexi; ILGP = inferior left GP; IRGP = inferior right GP; LAA = left atrial appendage; LIPV = left inferior pulmonary vein; LL = left lateral; LSPV = left superior pulmonary vein; MGP = Marshall GP; PA = posterior anterior; RIPV = right inferior pulmonary vein; RSPV = right superior pulmonary vein; SLGP = superior left GP.*
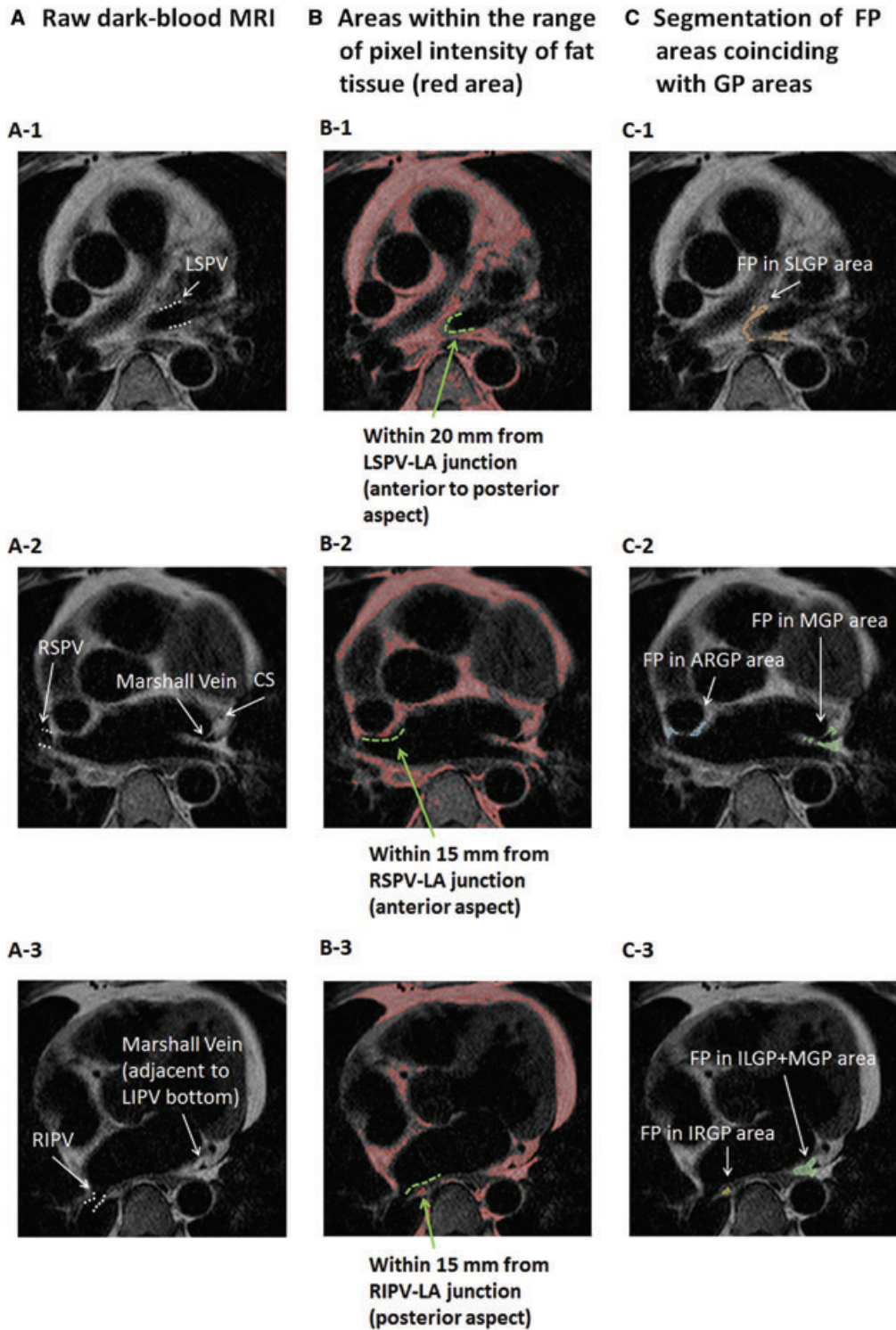
schematic images in Figure 1. SLGP area (red cross-mark) was defined as the area within 20 mm LA side from the anterior, superior, and posterior aspect of LSPV-LA junction. ILGP area (green cross-mark) was defined as the area within 15 mm LA side from the inferoposterior aspect of left inferior pulmonary vein (LIPV)-LA junction. ARGP area (blue cross-mark) was defined as the area within 15 mm LA side from the anterior aspect of right superior pulmonary vein (RSPV)-LA junction. IRGP area (yellow cross-mark) was defined as the area within 15 mm LA side from the inferoposterior aspect of right inferior pulmonary vein (RIPV)-LA junction. MGP area (purple cross-

mark) was defined as the area surrounding the Marshall Vein, which begins from the bottom of LIPV and extends into the ridge between LSPV and left atrial appendage (LAA).

Segmentation of FP Area Containing GP

Epicardial fat surrounding the LA can be recognized as bright regions in dark-blood MRI (Fig. 2A). The range of pixel intensities signifying LA epicardial fat were determined by sampling at least 20 points of pixel intensities in the large regions of subcutaneous fat and ventricular epicardial fat using the Corview segmentation

A Raw dark-blood MRI

B Areas within the range of pixel intensity of fat tissue (red area)

C Segmentation of FP areas coinciding with GP areas

A-1

B-1

C-1

LSPV

FP in SLGP area

Within 20 mm from LSPV-LA junction (anterior to posterior aspect)

A-2

B-2

C-2

RSPV

Marshall Vein   CS

FP in MGP area

FP in ARGP area

Within 15 mm from RSPV-LA junction (anterior aspect)

A-3

B-3

C-3

Marshall Vein (adjacent to LIPV bottom)

RIPV

FP in ILGP+MGP area

FP in IRGP area

Within 15 mm from RIPV-LA junction (posterior aspect)

Figure 2. *(A) Raw dark-blood MRI scans. (B) Red areas show the area within the range of the pixel intensity of fat tissue. (C) A subset of the FP regions, which coincided with anatomical GP locations were manually segmented from red areas. ARGP = anterior right GP; GP = ganglionated plexi; ILGP = inferior left GP; IRGP = inferior right GP; LA = left atrium; LIPV = left inferior pulmonary vein; LSPV = left superior pulmonary vein; MGP = Marshall GP; RIPV = right inferior pulmonary vein; RSPV = right superior pulmonary vein; SLGP = superior left GP.*

software. Areas which fell within that range of pixel intensities were highlighted using threshold tool (Fig. 2B). A subset of the fat tissue, which coincided with GP regions in the anatomical locations described above, were then manually segmented (Fig. 2C). These FP areas were considered as GP areas around LA.

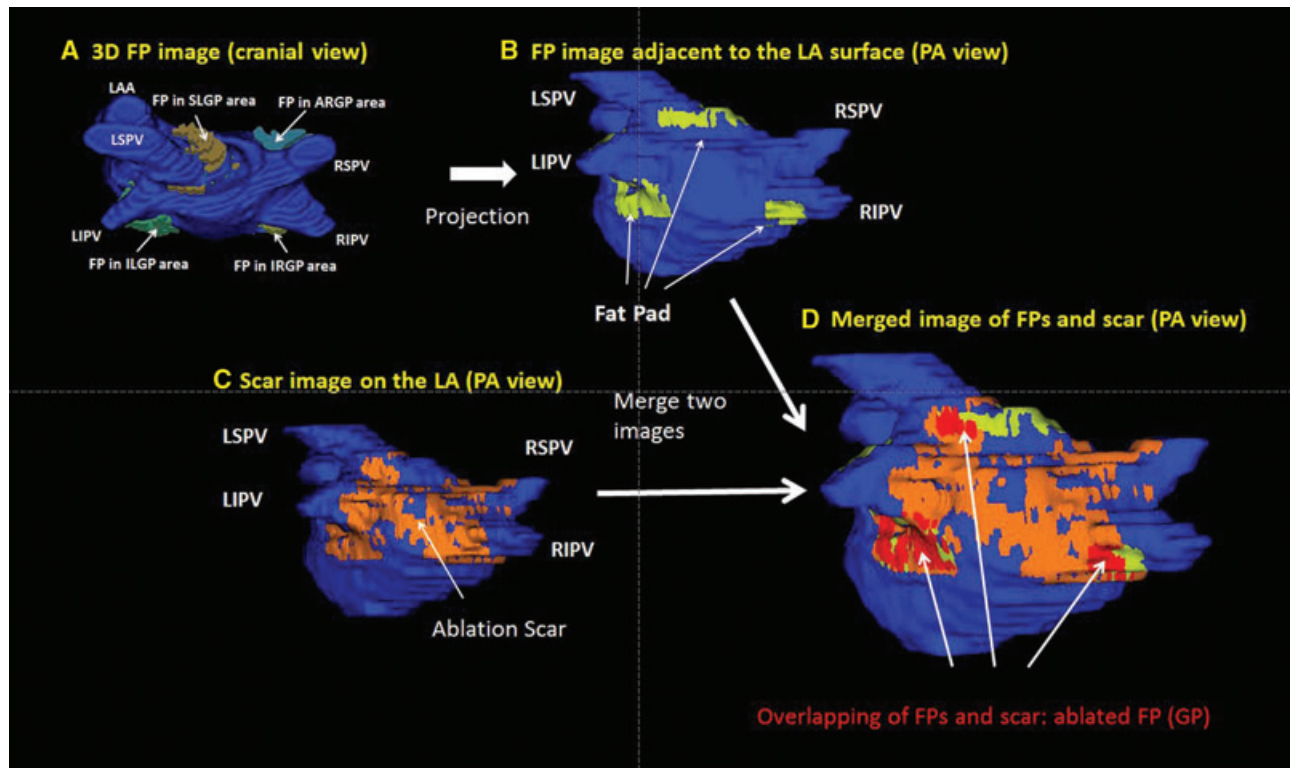### Merging LA, Scar, and FP Image

Segmented FPs were reconstructed as a 3D image on the LA (Fig. 3A), and then FPs adjacent to the LA surface were projected onto the LA surface (Fig. 3B). Subsequently, FPs image on the LA (Fig. 3B) was merged with the ablation scar image on the LA, which was visualized by LGE-MRI (Fig. 3C). Overlapping of FP areas and the ablation scar image were considered as ablated FP areas (Fig. 3D). And then the area of (1) entire LA surface, (2) ablation scar on the LA, and (3) ablated FP area were calculated. All these processes were executed using SCIRun software package, developed at the Scientific Computing

and Imaging (SCI) Institute at the University of Utah.

Holter Monitoring and Heart Rate Variability, Postablation Follow-Up

One-day postablation, 24-hour Holter monitoring was performed to obtain heart rate variability (HRV) measurements. We calculated percentage of differences greater than 50 ms in the RR intervals (pRR > 50) and standard deviation of RR intervals over the entire analyzed period (SDNN) as standard indicators of ANS activity after AF ablation.

A postablation-blanking period was observed for 3 months during which all patients received an 8-week automatic trigger cardiac event monitor for assessment of early AF recurrence. Early recurrences were treated with direct current cardioversion, antiarrhythmic drugs (AADs), or both. AADs were discontinued at the end of the blanking period. After blanking period, all patients were seen in the clinic at 3 months following

Figure 3. *Segmented FPs were reconstructed as a 3D image on the LA (A), and FPs adjacent to the LA surface were projected on the LA (B). Subsequently, FPs image on the LA (B) was merged with the ablation scar image on the LA (C). Overlapping of FP and ablation scar was considered as ablated FPs (GP) (D). ARGP = anterior right GP; FP = fat pad; GP = ganglionated plexi; ILGP = inferior left GP; IRGP = inferior right GP; LA = left atrium; LAA = left atrial appendage; LIPV = left inferior pulmonary vein; LSPV = left superior pulmonary vein; PA = posterior anterior; RIPV = right inferior pulmonary vein; RSPV = right superior pulmonary vein; SLGP = superior left GP.*

Table I.

Baseline Characteristic of Patients

	Total Patients (n = 60)	No Recurrence (n = 34)	Recurrence (n = 26)	P Value
Age, years	65 ± 13	62 ± 14	70 ± 9	0.01*
Gender, male/female, n	35/25	21/13	14/12	0.60
HTN, n	34	17	17	0.30
DM, n	11	5	6	0.51
CAD, n	14	7	7	0.76
CABG, n	3	1	2	0.57
MI, n	4	1	3	0.30
CHF, n	3	1	2	0.57
Cardiomyopathy, n	3	3	0	0.25
Implantable device, n	2	1	1	1.00
Stroke, n	6	2	4	0.39
Smoking, n	21	10	11	0.41
AF Type				
Paroxysmal, n	32	20	12	0.33
Persistent, n	28	14	14	0.33

*$P < 0.05$. No recurrence versus recurrence.
CABG = coronary artery bypass graft; CAD = coronary artery disease; CHF = congestive heart failure; DM = diabetes mellitus; HTN = hypertension; MI = myocardial infarction.

ablation and followed-up at 3-month intervals thereafter until 12-month postablation.

Each patient received a 12-lead ECG at every visit. Additional ECG recordings and 24-hour Holter monitorings were obtained as suggested by the patients' symptoms. Recurrence was defined as any atrial arrhythmia sustained for longer than 30 seconds without AAD treatment following blanking period.

Statistics and Analysis

Continuous variables are presented as mean ± standard deviation. Statistical comparisons were performed with Student's t-test, Fisher's exact test, or χ^2 analysis, as appropriate. A probability value of $P < 0.05$ was considered to be statistically significant.

Results
Patient Characteristics and Ablation Results

All 60 patients (35 male; mean age 65 ± 13 years) underwent AF ablation, and no LA-PV conduction was recognized after PVA isolation. All patients were followed until 12-month postablation, and out of 60 patients, 34 patients (57%) remained in normal sinus rhythm while the remaining 26 patients (43%) experienced a recurrence of AF after the 3-month blanking period following the initial AF ablation. Patients with recurrence were significantly older

than those without recurrence. However, there were no significant differences between these two groups regarding other baseline characteristics, including AF type (Table I).

Scar area, FP Area, and Overlapping of these Areas

LA surface area, the total postablation scar area, each FP area, and the overlapping of scar area and FP area (i.e., ablated FP area) are shown in Table II. There were no significant differences in LA surface area (184.0 ± 31.9 cm^2 vs 198.5 ± 45.3 cm^2; P = 0.15), the total postablation scar area (22.5 ± 8.2 cm^2 vs 21.2 ± 12.7 cm^2; P = 0.65), and each FP area (9.6 ± 3.7 cm^2 vs 10.3 ± 3.9 cm^2; P = 0.28 [SLGP area], 7.6 ± 4.1 cm^2 vs 9.0 ± 3.9 cm^2; P = 0.17 [ILGP+MGP area], 5.7 ± 2.9 cm^2 vs 5.5 ± 3.3 cm^2; P = 0.80 [ARGP area], 2.4 ± 1.6 cm^2 vs 2.7 ± 2.3 cm^2; P = 0.50 [IRGP area]) between patients without and with recurrence. We noticed a significant difference in the ablated FP area between patients without and with recurrence in all regions except for IRGP area (1.6 ± 1.5 cm^2 vs 1.0 ± 0.9 cm^2; P = 0.04 [SLGP area], 2.1 ± 1.3 cm^2 vs 1.5 ± 1.1 cm^2; P = 0.03 [ILGP + MGP area], 1.2 ± 0.6 cm^2 vs 0.7 ± 0.6 cm^2; P = 0.01 [ARGP area], 0.7 ± 0.8 cm^2 vs 0.9 ± 1.2 cm^2; P = 0.21 [IRGP area]). In addition, the total ablated FP was significantly wider in patients without recurrence

Table II.

Scar Area, FP Area, and These Overlap Areas

	No Recurrence (n = 34)	Recurrence (n = 26)	P Value
LA surface (cm^2)	184.0 ± 31.9	198.5 ± 45.3	0.15
Total scar area (cm^2)	22.5 ± 8.2	21.2 ± 12.7	0.65
FP Area (cm^2)			
SLGP area	9.6 ± 3.7	10.3 ± 3.9	0.28
ILGP + MGP area	7.6 ± 4.1	9.0 ± 3.9	0.17
ARGP area	5.7 ± 2.9	5.5 ± 3.3	0.80
IRGP area	2.4 ± 1.6	2.7 ± 2.3	0.50
Total	25.2 ± 9.0	27.5 ± 9.2	0.33
Ablated FP (cm^2)			
SLGP area	1.6 ± 1.5*	1.0 ± 0.9*	0.04*
ILGP + MGP area	2.1 ± 1.3*	1.5 ± 1.1*	0.03*
ARGP area	1.2 ± 0.6*	0.7 ± 0.6*	0.01*
IRGP area	0.7 ± 0.8	0.9 ± 1.2	0.21
Total	5.6 ± 3.1*	4.2 ± 2.7*	0.03*

*P < 0.05. No recurrence versus recurrence.
ARGP = anterior right GP; FP = fat pad; GP = ganglionated plexi; ILGP = inferior left GP; IRGP = inferior right GP; LA = left atrium; MGP = Marshall GP; SLGP = superior left GP.

compared to those in patients with recurrence (5.6 ± 3.1 cm^2 vs 4.2 ± 2.7 cm^2; P = 0.03).

Ablation Effects to HRV

Patients underwent a 24-hour Holter monitoring 1-day post-AF ablation. During this monitoring period, AF episodes were documented in four patients and frequent atrial paroxysmal beats (over 15% of the whole day) were observed in two patients. Therefore these six patients were excluded from the analysis, and HRV data from remaining 54 patients (No recurrence: 31 patients, Recurrence: 23 patients) were used. Maximum heart rate, minimum heart rate, mean heart rate, pRR > 50, and SDNN were obtained from the 24-hour Holter monitoring (Table III). The mean values of both pRR > 50 and SDNN in patients without recurrence were significantly lower than those in patients with recurrence (5.8 ± 6.0% vs 14.0 ± 10.1%; P = 0.0005, 78.7 ± 32.4 ms vs 109.2 ± 43.5 ms; P = 0.005, Table III) 1-day post-AF ablation. There was also a significant negative correlation between SDNN and the percentage of ablated total FP area (Y = −1.3168X + 118.96, R^2 = 0.1576, P = 0.003, Fig. 4) indicating a decrease in autonomic nerve activity corresponding to an increase of ablated FP area.

Table III.

HR and HRV Data after Ablation

	No Recurrence (n = 31)	Recurrence (n = 23)	P Value
Max HR (beats/min)	107.7 ± 18.5	104.9 ± 23.0	0.66
Min HR (beats/min)	61.6 ± 8.0	54.0 ± 9.0	0.006*
Mean HR (beats/min)	76.6 ± 9.4	75.9 ± 10.9	0.83
pRR>50 (%)	5.8 ± 6.0	14.0 ± 10.1	0.0005*
SDNN (ms)	78.7 ± 32.4	109.2 ± 43.5	0.005*

*P < 0.05. No recurrence versus recurrence.
HR = heart rate; HRV = heart rate variability; pRR > 50 = percentage of differences higher than 50 ms in RR intervals; SDNN = standard deviation of RR intervals over the entire analyzed period.

Discussion

In this study using LGE-MRI and dark-blood MRI, based on merging ablation scar image and the image of FP area containing GP, we demonstrated significant correlations between ablated total FP area, autonomic denervation, and AF prognosis. FP area was ablated wider in patients without recurrence of AF than in patients with recurrence even though total ablation area (total scar area) and total FP area were not significantly different between both groups (the schema was shown in Fig. 5). It means that, as previously suggested,
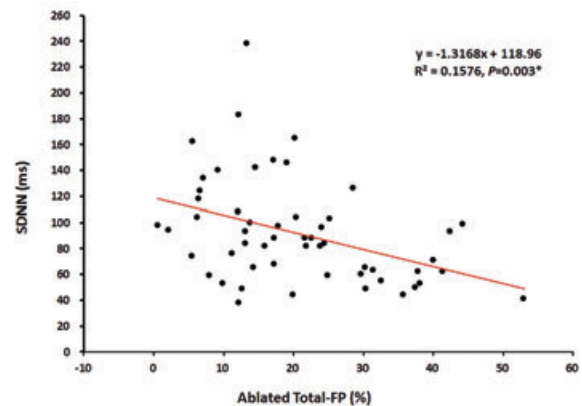
Figure 4. *This figure shows the relationship between SDNN and the percentage of ablated total FP area. There was a significant negative correlation between two values. FP = fat pad; SDNN = standard deviation of RR intervals over the entire analyzed period.*
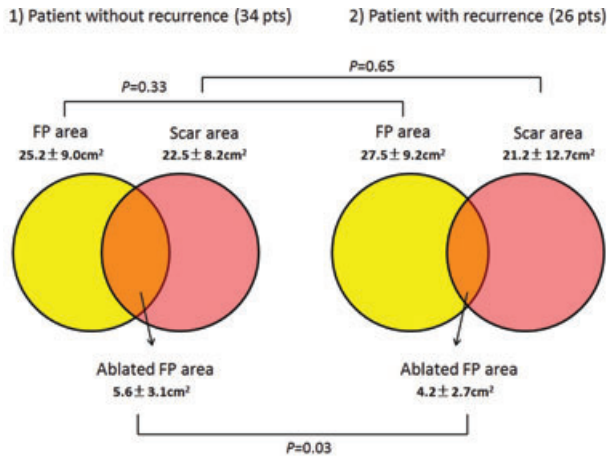
Figure 5. *This schema shows that FP area was ablated wider in patients without recurrence of AF than in patients with AF recurrence even though total ablation scar area and total FP area were not different between both groups. FP = fat pad.*

targeting and ablating wider FP areas containing GP area in addition to PVI would result in denervation of ANS and ultimately improve the AF prognosis after ablation.

Previous Studies

Epicardial GP are mainly distributed at specific regions and are primarily distributed within the epicardial FP.[22] The critical role of GP in the dynamics of AF initiation and maintenance has been demonstrated in many reports and the effect of GP ablation on attenuating AF inducibility is widely accepted nowadays.[26–29] During the routine PVA isolation procedure, some of the GP regions are automatically included in the ablation lesions owing to the anatomical location of GP regions. Pappone et al.[16] demonstrated that inadvertent modification of GP during PVA isolation improved outcome post-AF ablation. Hence, we sought to demonstrate the impact of inadvertent FP ablation on the prognosis of AF after routine AF ablation using noninvasive LGE-MRI modality.

Definition and Segmentation of GP Areas

To locate and segment GP areas, we cautiously followed the anatomical instructions provided in previous studies.[11,14,15,19–24,30] Tan et al.[24] reported in their histological study that autonomic innervations were recognized mainly within 10-mm LA side from the each PV-LA junction. Katritsis et al.[15] defined presumed GP areas as within 10–20 mm LA side from the PV-LA junctions in their study. Po et al.[14] described in

their study that the ILGP and IRGP are located 1–3 cm below the LIPV and RIPV, respectively. In addition, Scanavacca et al.[25] demonstrated the vagal response during applying the HFS on the posterior aspect of LSPV-LA junction. Our definition of certain GP areas in this study is the average of these anatomical instructions from histological and clinical reports.

Regarding Marshall GP, we could identify the distinct Marshall Vein running into the FP at the anterior surface of left PV-LA junction in the MRI as shown in Figure 2. We could easily segment FP around the Marshall Vein. Makino et al.[19] reported that 25 of 26 postmortem human hearts had a Marshall bundle which accompanied the GP located around the Marshall Vein.

Autonomic Denervation after Ablation and Its Influence on AF Prognosis

We identified a significant negative correlation between SDNN and ablated total-FP area, strongly suggesting that the autonomic nerve activity was suppressed with increase in the net ablated FP area. We also demonstrated that the mean values of both pRR > 50 and SDNN were significantly lower in patients without recurrence than those in patients with recurrence, suggesting a greater reduction in autonomic nerve activity in patients without AF recurrence.

Pokushalov et al.[30] demonstrated, in comparison with the conventional approach using HFS, the significant superiority of anatomical GP ablation in terms of the autonomic denervation as well as AF prognosis after ablation (follow-up period was 13.1 ± 1.9 months). They mentioned that HFS at a particular site might elicit the parasympathetic response by stimulating not the autonomic ganglia itself but the autonomic nerves in the neural network of ANS. They also mentioned that the response to HFS is dependent on the property of AV node; therefore, HFS is not a fully reliable method to confirm GP area. They concluded that the promising technique of GP ablation is to ablate anatomical GP regions extensively without searching GP area by HFS.

Long-term outcome of GP ablation itself is still controversial. In a study of Oh et al.,[31] long-term effect of GP ablation was assessed using experimental mongrel dogs. The vagal denervation and the suppression of AF inducibility were observed immediately after the ablation of right pulmonary vein FP and the inferior vena cava-left atrium FP, but these effects disappeared after 4 weeks. However this attenuation of denervation was considered to be attributed to the incompleteness of ablating FP containing GP.[32,33] In other words, FP of every GP location should be extensively ablated to diminish the

number of GP inside FP and to maximize the denervation because some part of fat in GP lesion does not contain autonomic ganglia. In addition, if some GP regions are left untreated, it may lead rather increase vulnerability and enhance AF inducibility.[34]

When comparing GP ablation and PVI, the report of Mikhaylov et al.[35] is interesting. In this study, anatomic GP ablation for paroxysmal AF patients showed a significantly lower success rate over a 3-year follow-up period compared with circumferential PVI (34.3% vs 65.7%, respectively; P = 0.008). There is another study by Katritsis et al.[15] reporting the result of anatomical GP ablation as an adjunctive therapy with PVI. In this study, patients who underwent anatomical GP ablation in addition to PVI had significantly better arrhythmia-free survival compared with patients who underwent only PVI. These two reports are suggesting that GP ablation itself yields to PVI and GP ablation should be combined with PVI.

Summarizing resent studies, we should consider the following issues to maximize the effect of GP ablation; (1) FP of GP location should be ablated anatomically and extensively, (2) all GP locations should be ablated; otherwise it can rather enhance the AF inducibility, and (3) PVI should be performed in addition to GP ablation.

In this study, we demonstrated by means of LGE-MRI the same concept as described above that the extensive ablation of FP in every anatomical GP location in addition to PVI leads denervation of ANS and ultimately improve the AF prognosis after ablation.

Study Limitations

We acknowledge that the main limitation of this study is that GP cannot be located readily from MRI image and we used FP as a surrogate of GP by anatomical reference. However, we cautiously followed previously published studies that have defined the anatomical locations of GP around the LA. We also have to acknowledge that this study is a retrospective study and includes a small number of patients. Therefore a prospective study with large number of subjects targeting FP area containing GP along with PVI should be performed to confirm this result. However, this is the first study that evaluated the impact of ablation to FP containing GP during AF ablation using noninvasive LGE-MRI modality.

Conclusion

Extensively ablating FP regions containing GP area in addition to PVI enhanced the denervation of ANS and seemed to improve procedural outcome in patients with AF. These results were successfully demonstrated using LGE-MRI.

References

1. Haïssaguerre M, Jaïs P, Shah DC, Takahashi A, Hocini M, Quiniou G, Garrigue S, et al. Spontaneous initiation of atrial fibrillation by ectopic beats originating in the pulmonary veins. New Eng J Med 1998; 339:659–666.
2. Pappone C, Oreto G, Rosanio S, Vicedomini G, Tocchi M, Gugliotta F, Salvati A, et al. Atrial electroanatomic remodeling after circumferential radiofrequency pulmonary vein ablation: Efficacy of an anatomic approach in a large cohort of patients with atrial fibrillation. Circulation 2001; 104:2539–2544.
3. McGann CJ, Kholmovski EG, Oakes RS, Blauer JJE, Daccarett M, Segerson N, Airey KJ, et al. New magnetic resonance imaging-based method for defining the extent of left atrial wall injury after the ablation of atrial fibrillation. J Am Coll Cardiol 2008; 52:1263–1271.
4. Badger TJ, Oakes RS, Daccarett M, Burgon NS, Akoum N, Fish EN, Blauer JJE, et al. Temporal left atrial lesion formation after ablation of atrial fibrillation. Heart Rhythm 2009; 6:161–168.
5. Reddy VY, Schmidt EJ, Holmvang G, Fung M. Arrhythmia recurrence after atrial fibrillation ablation: Can magnetic resonance imaging identify gaps in atrial ablation lines? J Cardiovasc Electrophysiol 2008; 19:434–437.
6. Peters DC, Wylie JV, Hauser TH, Kissinger KV, Botnar RM, Essebag V, Josephson ME, et al. Detection of pulmonary vein and left atrial scar after catheter ablation with three-dimensional navigator-gated delayed enhancement mr imaging: Initial experience. Radiology 2007; 243:690–695.
7. Kim RJ, Wu E, Rafael A, Chen EL, Parker MA, Simonetti O, Klocke FJ, et al. The use of contrast-enhanced magnetic resonance imaging to identify reversible myocardial dysfunction. N Engl J Med 2000; 343:1445–1453.
8. De Cobelli F, Pieroni M, Esposito A, Chimenti C, Belloni E, Mellone R, Canu T, et al. Delayed gadolinium-enhanced cardiac magnetic resonance in patients with chronic myocarditis presenting with heart failure or recurrent arrhythmias. J Am Coll Cardiol 2006; 47:1649–1654.
9. Schauerte P, Scherlag BJ, Pitha J, Scherlag MA, Reynolds D, Lazzara R, Jackman WM. Catheter ablation of cardiac autonomic nerves for prevention of vagal atrial fibrillation. Circulation 2000; 102:2774–2780.
10. Hou Y, Scherlag BJ, Lin J, Zhang Y, Lu Z, Truong K, Patterson E, et al. Ganglionated plexi modulate extrinsic cardiac autonomic nerve input: Effects on sinus rate, atrioventricular conduction, refractoriness, and inducibility of atrial fibrillation. J Am Coll Cardiol 2007; 50:61–68.
11. Mehall JR, Kohut RMJ, Schneeberger EW, Taketani T, Merrill WH, Wolf RK. Intraoperative epicardial electrophysiologic mapping and isolation of autonomic ganglionic plexi. Ann Thorac Surg 2007; 83:538–541.
12. Lemola K, Chartier D, Yeh YH, Dubuc M, Cartier R, Armour A, Ting M, et al. Pulmonary vein region ablation in experimental vagal atrial fibrillation: Role of pulmonary veins versus autonomic ganglia. Circulation 2008; 117:470–477.
13. Sakamoto S, Schuessler RB, Lee AM, Aziz A, Lall SC, Damiano RJJ. Vagal denervation and reinnervation after ablation of ganglionated plexi. J Thorac Cardiovasc Surg 2010; 139:444–452.
14. Po SS, Nakagawa H, Jackman WM. Localization of left atrial ganglionated plexi in patients with atrial fibrillation. J Cardiovasc Electrophysiol 2009; 20:1186–1189.
15. Katritsis DG, Giazitzoglou E, Zografos T, Pokushalov E, Po SS, Camm AJ. Rapid pulmonary vein isolation combined with autonomic ganglia modification: A randomized study. Heart Rhythm 2011; 8:672–678.
16. Pappone C, Santinelli V, Manguso F, Vicedomini G, Gugliotta F, Augello G, Mazzone P, et al. Pulmonary vein denervation enhances long-term benefit after circumferential ablation for paroxysmal atrial fibrillation. Circulation 2004; 109:327–334.

17. Akoum N, Daccarett M, McGann C, Segerson N, Vergara G, Kuppahally S, Badger T, et al. Atrial fibrosis helps select the appropriate patient and strategy in catheter ablation of atrial fibrillation: A DE-MRI guided approach. J Cardiovasc Electrophysiol 2011; 22:16–22.

18. Mahnkopf C, Badger TJ, Burgon NS, Daccarett M, Haslam TS, Badger CT, McGann CJ, et al. Evaluation of the left atrial substrate in patients with lone atrial fibrillation using delayed-enhanced MRI: Implications for disease progression and response to catheter ablation. Heart Rhythm 2010; 7:1475–1481.

19. Makino M, Inoue S, Matsuyama T, Ogawa G, Sakai T, Kobayashi Y, Katagiri T, et al. Diverse myocardial extension and autonomic innervation on ligament of Marshall in humans. J Cardiovasc Electrophysiol 2006; 17:594–599.

20. Valderrabano M, Chen HR, Sidhu J, Rao L, Ling Y, Khoury DS. Retrograde ethanol infusion in the vein of marshall: Regional left atrial ablation, vagal denervation and feasibility in humans. Circ Arrhythm Electrophysiol 2009; 2:50–56.

21. Katritsis D, Giazitzoglou E, Sougiannis D, Goumas N, Paxinos G, Camm AJ. Anatomic approach for ganglionic plexi ablation in patients with paroxysmal atrial fibrillation. Am J Cardiol 2008; 102:330–334.

22. Armour JA, Murphy DA, Yuan BX, MacDonald S, Hopkins DA. Gross and microscopic anatomy of the human intrinsic cardiac nervous system. Anat Rec 1997; 247:289–298.

23. Cummings JE, Gill I, Akhrass R, Dery M, Biblo LA, Quan KJ. Preservation of the anterior fat pad paradoxically decreases the incidence of postoperative atrial fibrillation in humans. J Am Coll Cardiol 2004; 43:994–1000.

24. Tan AY, Li H, Wachsmann-Hogiu S, Chen LS, Chen PS, Fishbein MC. Autonomic innervation and segmental muscular disconnections at the human pulmonary vein-atrial junction: Implications for catheter ablation of atrial-pulmonary vein junction. J Am Coll Cardiol 2006; 48:132–143.

25. Scanavacca M, Pisani CF, Hachul D, Lara S, Hardy C, Darrieux F, Trombetta I, et al. Selective atrial vagal denervation guided by evoked vagal reflex to treat patients with paroxysmal atrial fibrillation. Circulation 2006; 114:876–885.

26. Scherlag BJ, Nakagawa H, Jackman WM, Yamanashi WS, Patterson E, Po SS, Lazzara R. Electrical stimulation to identify neural elements on the heart: Their role in atrial fibrillation. J Interv Card Electrophysiol 2005; 13:37–42.

27. Scherlag BJ, Yamanashi W, Patel U, Lazzara R, Jackman WM. Autonomically induced conversion of pulmonary vein focal firing into atrial fibrillation. J Am Coll Cardiol 2005; 45:1878–1886.

28. Lemola K, Chartier D, Yeh YH, Dubuc M, Cartier R, Armour A, Ting M, et al. Pulmonary vein region ablation in experimental vagal atrial fibrillation: Role of pulmonary veins versus autonomic ganglia. Circulation 2008; 117:470–477.

29. Lu Z, Scherlag BJ, Lin J, Yu L, Guo JH, Niu G, Jackman WM, et al. Autonomic mechanism for initiation of rapid firing from atria and pulmonary veins: Evidence by ablation of ganglionated plexi. Cardiovasc Res 2009; 84:245–252.

30. Pokushalov E, Romanov A, Shugayev P, Artyomenko S, Shirokova N, Turov A, Katritsis DG. Selective ganglionated plexi ablation for paroxysmal atrial fibrillation. Heart Rhythm 2009; 6:1257–1264.

31. Oh S, Zhang Y, Bibevski S, Marrouche NF, Natale A, Mazgalev TN. Vagal denervation and atrial fibrillation inducibility: Epicardial fat pad ablation does not have long-term effects. Heart Rhythm 2006; 3:701–708.

32. Scherlag B. Re: Vagal denervation and atrial fibrillation inducibility: Epicardial fat pad ablation does not have long-term effects. Heart Rhythm 2006; 3:1248–1249.

33. Mounsey JP. Recovery from vagal denervation and atrial fibrillation inducibility: Effects are complex and not always predictable. Heart Rhythm 2006; 3:709–710.

34. Hirose M, Leatmanoratn Z, Laurita KR, Carlson MD. Partial vagal denervation increases vulnerability to vagally induced atrial fibrillation. J of Cardiovasc Electrophysiol 2002; 13:1272–1279.

35. Mikhaylov E, Kanidieva A, Sviridova N, Abramov M, Gureev S, Szili-Torok T, Lebedev D. Outcome of anatomic ganglionated plexi ablation to treat paroxysmal atrial fibrillation: A 3-year follow-up study. Europace 2011; 13:362–370.